https://doi.org/10.5194/egusphere-2025-6265
Preprint. Discussion started: 6 January 2026

Brief communication: Three dimensional modelling of surface waves generated by shallow submarine volcanic eruptions

Manish Kanojia*[1]

[1]Institute of Coastal Systems-Analysis and Modeling, Helmholtz-Zentrum Hereon, 21502 Geesthacht , Germany

Abstract

This study investigates the generation of surface waves during shallow submarine volcanic eruptions by incorporating a Gaussian heat flux at the seabed to simulate eruption dynamics. Using the three-dimensional ocean flow model PSOM, we analyzed wave generation mechanisms under varying heat flux levels (10,000 W/m^2 and 20,000 W/m^2) and volcanic depths. Results demonstrate that higher heat flux values and shallower eruption depths produce larger surface waves, corroborating findings from prior research. By modeling the heat flux-driven convection flows, including plume generation and water entrainment, the study highlights the critical role of thermal effects in tsunami formation. The proposed methodology enhances traditional tsunami models by accounting for heat flux impacts on vertical velocity and surface displacement. These findings provide new insights into the hazards posed by shallow submarine eruptions, improving risk assessments for coastal regions.

1 Introduction

Substantial submarine volcanic eruptions occurring within the top 500 meters from the water's surface are likely to produce waves on the surface [Kanojia et al., 2023, Paris et al., 2014]. Traditional tsunami generation models employ a displacement potential function to account for the initial displacement caused by seismic or non-seismic events at the sea surface. This approach incorporates the addition of mass flux or seabed displacement due to various factors such as landslides or other geological activities. However, submarine volcanic eruptions not only introduce mass to the system but also generate a significant heat flux which is the focus of this paper. The heat flux causes convection flows driven by buoyant forces acting on the high-temperature, less dense water near the volcano. Consequently, this results in the upward movement of water. In a shallow environment with substantial heat flux, this vertical flow can penetrate the free surface and generate surface waves. Incorporating the heat flux introduces high temperatures near the volcano and includes the phenomenon of plume generation and the entrainment of water into the plume. This affects the vertical velocity, consequently impacting the generation of the surface waves.

The tsunami generation process is complex but can be summarized as follows: As the volcano erupts, it forces an initial upward movement of the water column directly above the site of the eruption. This sudden displacement creates a dome-shaped structure on the ocean's surface, a visible bulge formed by the rapid rise of water. Following the initial uplift, the water that was forced upward begins to collapse back. This collapse results in the formation of a trough directly above the volcanic site. The water rushes back down, creating a localized depression in the ocean surface. From this trough, waves start to propagate outward in all directions. The energy from the eruption causes these waves to travel rapidly across the ocean surface. As they move away from the trough, the waves grow in height and spread out [Le Méhauté and Wang, 1996, Torsvik et al., 2010, Paris, 2015, Paris and Ulvrova, 2019, Kedrinskii, 2005, Morrissey et al., 2010, Nakano et al., 1954, Moore et al., 1966, Muraviev et al., 1998, Nishimura et al., 2005]. Some of the recent studies [Liu and Fritz, 2023, Schindelé et al., 2024] also discuss the same mechanism for surface wave generation due to submarine volcanic eruptions.

*Email: kanojiam@tcd.ie

https://doi.org/10.5194/egusphere-2025-6265
Preprint. Discussion started: 6 January 2026

We will utilize the three-dimensional ocean flow model PSOM [Mahadevan et al., 1996b, Mahadevan et al., 1996a] to examine the surface waves generated by the introduction of a high heat flux at the seabed in a shallow environment. A Gaussian heat flux profile will be applied at the seabed with significant heat flux values. We will investigate two different heat flux levels ($10000, 20000$ watts/m^2) at the seabed and compare the resulting surface waves. Additionally, we will analyze the surface elevation for the cases with different depth of volcano from free surface. This analysis aims to identify the best-case scenario for shallow volcanoes near the coast, which could potentially cause damage to infrastructure and coastal communities.

2 Model parameters and initial conditions

The domain's dimensions are 30 kilometers in both the x and y directions. Mean salinity $S_0 = 35.70$ ppt, mean temperature $T_0 = 15°\text{C}$ and mean density $\rho_0 = 1027$ kg/m^3. The value of earth's angular velocity is 7.272×10^{-5} rad/sec, the magnitude of Coriolis parameter is 10^{-4} rad/sec, the acceleration due to gravity on the surface of the earth at sea level is 9.81 m/s^2, value of Earth's radius is 6371 km. The grid dimensions are as follows $NI = 128, NJ = 128$, and $NK = 36$ in x, y and z dimensions respectively. The diffusion and viscosity in both the horizontal x and y directions is 2 m^2/s and vertical diffusion is 10^{-5} m^2/s. Damping has been implemented at the boundaries to prevent reflections generated when the flow reaches the perimeter.

The flux at two lateral boundaries is considered to be zero.

Due to heat flux at the bottom boundary we introduce the boundary condition at seabed as

$$\kappa \frac{\partial T}{\partial z} = \frac{Q}{\rho C_p}, \tag{1}$$

where Q is specified heat flux at the bottom boundary, C_p is the specific heat capacity.

At the time $t = 0$, the velocities u, v, and w are all initialized to zero, meaning the water is initially motionless.

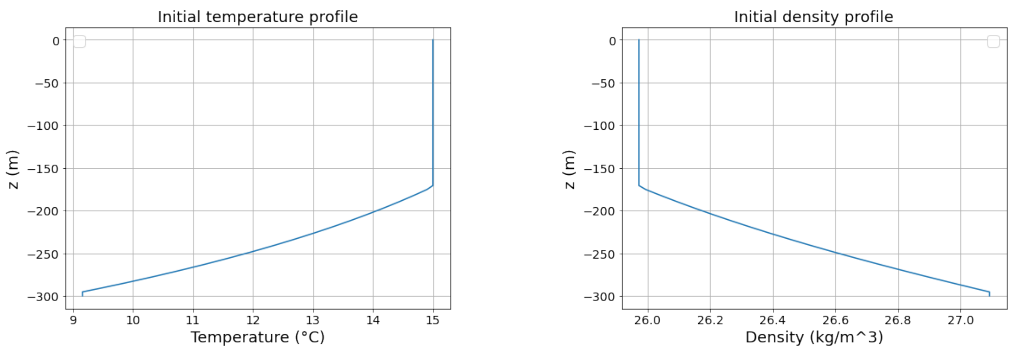

(a) Initial temperature (b) Initial density

Figure 1: Plots for initial temperature and density profile.

3 Results

3.1 Case 1: Heat flux $20,000$ watts/m^2

A Gaussian heat flux profile was applied to the seabed, with the peak heat flux reaching $20,000$ watts per square meter at the coordinates $(x, y) = (0, 0)$ and gradually decreasing to zero in both directions.

Figure 2 (a) illustrates that one minute after the eruption begins, a dome-shaped structure forms on the free surface. Following this, the vertical dome undergoes a gravity collapse, creating a trough from which waves propagate outward on both sides (see Figure. 2 (b)-(d)), as discussed in [Liu and Fritz, 2023, Schindelé et al., 2024]. Figure 2 (b)-(d) demonstrate that with the continuous addition of heat flux at

https://doi.org/10.5194/egusphere-2025-6265
Preprint. Discussion started: 6 January 2026

the seabed, the surface elevation increases, reaching approximately 1 meter at $t = 11$ minutes and 2 meters at $t = 13$ minutes. Additionally, these figures show that as the heat flux continues to be added and the wave elevation rises, the domain of influence of the waves on the surface expands. Specifically, in Figure 2 (b), at $t = 6$ minutes, the waves dissipate within a range of 5000 meters on both sides, with the elevation reaching zero at this distance. However, Figure. 2 (c) and (d) indicate that there is a positive elevation at 5000 meters from the source, with the elevation decreasing to zero around 6000 meters from the source in both directions.

3.2 Case 2: Heat flux $10,000$ watts/m^2

In this case, a Gaussian heat flux, peaking at 10000 watts/m^2 at the coordinates $(x, y) = (0, 0)$, was applied to the bottom boundary.

In case 2, the initial upward displacement of the surface is observed six minutes after the eruption. As more heat flux is added, the initial dome-like structure collapses due to gravity, forming a trough. Subsequently, waves begin to propagate outwards from both sides of the trough (see Figure 3 (a)-(d)). Even after 13 minutes post-eruption, the surface elevation remains minimal, with a maximum of 0.02 meters. However, with continuous heat flux input (eruption) for over 20 minutes, the surface elevation increases significantly, reaching approximately 1.5 meters at 24 minutes after the initial eruption. At this point, the influence of the surface waves extends up to a range of 5000 meters (see Figure 3 (d)).

3.3 Comparison of case 1 and 2

It should be noted that in case 1, a heat flux of $20,000$ watts/m^2 was introduced at the seabed. Due to the large energy input, the simulations were executed for 15 minutes to ensure numerical stability.

In both cases, the phenomenon of surface wave generation is consistent with the findings discussed in [Liu and Fritz, 2023, Schindelé et al., 2024]. However, higher elevations were observed in a shorter time span in case 1, where a larger heat flux was introduced at the seabed. This is because a larger heat flux rapidly heats the water around the volcano, increasing the temperature more significantly compared to case 2, for example after 6 minutes from the eruption the temperature near the volcano in case 1 was 600°C whereas in case 2 it was around 110°C (see Figure 4). Consequently, the water becomes less dense, resulting in a larger buoyant force. This causes the water to be convected upward more quickly, reaching the surface sooner and with higher impact velocity creating larger waves. It can further be noted from Figure 2 (d) and 3 (b) that at 13 minutes after the eruption the highest wave elevation in case 1 was 2 meters where as in case 2 it was around 0.03 meters.

The extent of the wave impact on the free surface varies between the two cases, despite observing nearly the same wave elevation. In the first case, when a two-meter wave was observed, the domain of influence extended approximately 6000 meters in both directions (see Figure 2 (d)). However, in the second case, with a nearly two-meter wave, the domain of influence was limited to within 5000 meters in both directions from the source (see Figure 3 (d)).

3.4 Comparison of the surface elevation with different depth values and fixed heat flux

For a fixed heat flux of 10,000 watts/m^2, the total depth of the system was reduced to 200 meters with heat flux at the seabed. This scenario corresponds to the crater of the volcano being closer to the free surface compared to case 2. In both cases, a constant heat flux was applied continuously for 24 minutes.

As depicted in Figure 6 (a) and 3 (a), six minutes after the eruption, an initial uplift with very small elevation was observed when the volcano was 300 meters from the free surface. In contrast, when the volcano was located 200 meters from the free surface, a trough and waves were observed six minutes after the eruption. Figure 5 (b) illustrates that 24 minutes after the eruption, a higher wave elevation was observed when the volcano was closer to the free surface. Specifically, a wave elevation of approximately 5 meters was recorded when the volcano was 200 meters from the free surface. In comparison, a wave elevation of approximately 1.7 meters was observed when the volcano was situated 300 meters from the free surface. These observations of increased wave elevation when the volcano is closer to the free surface have been corroborated in other studies [Lipiejko et al., 2021].

https://doi.org/10.5194/egusphere-2025-6265
Preprint. Discussion started: 6 January 2026

4 Remarks

In this paper, a Gaussian heat flux was applied to the seabed to simulate the surface waves generated by submarine volcanic eruptions. The study explored the mechanism behind surface wave generation during major shallow submarine volcanic eruptions by applying heat flux to the seabed and found a strong correlation with previous research [Liu and Fritz, 2023, Schindelé et al., 2024]. It was observed that larger waves resulted from higher heat flux values and when the heat source was closer to the water surface. These findings are consistent with earlier studies and observations, such as those reported in [Lipiejko et al., 2021]. This study proposes an alternative methodology for modeling tsunamis generated by submarine volcanic eruptions. By incorporating heat flux at the bottom boundary, the tsunami generation process accounts for the complex phenomena of vertical tephra transport (plume generation) and the entrainment of ambient seawater into the vertical plume, which impacts vertical velocity, as discussed in previous studies [Rossby, 1965, Rossby, 1998].

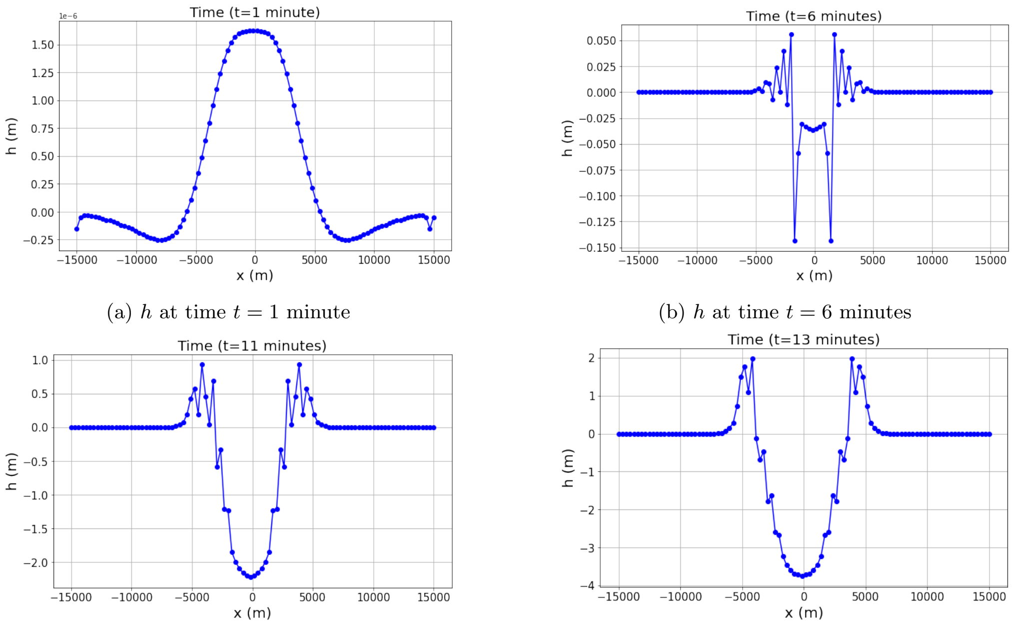

(a) h at time $t = 1$ minute
(b) h at time $t = 6$ minutes
(c) h at time $t = 11$ minutes
(d) h at time $t = 13$ minutes

Figure 2: Plots of h for case 1 at different times from the eruption.

https://doi.org/10.5194/egusphere-2025-6265
Preprint. Discussion started: 6 January 2026

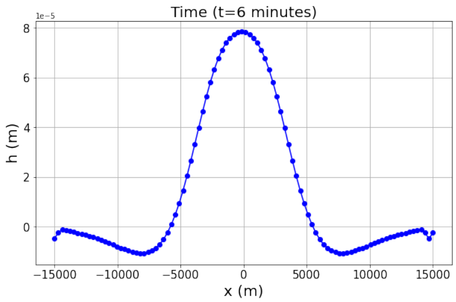

(a) h at time $t = 6$ minutes

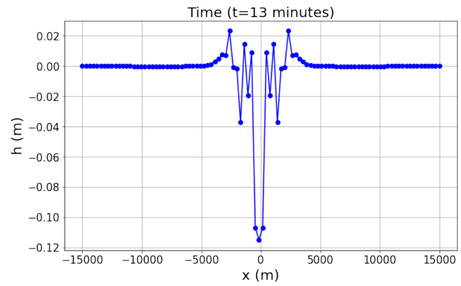

(b) h at time $t = 13$ minutes

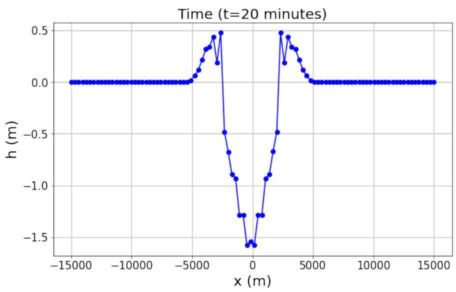

(c) h at time $t = 20$ minutes

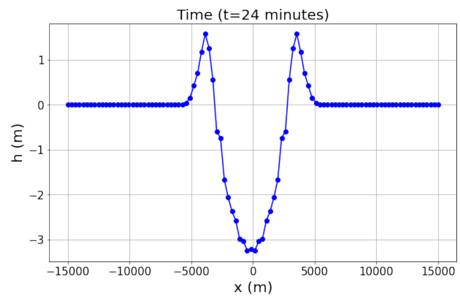

(d) h at time $t = 24$ minutes

Figure 3: Plots of h for case 2 at different times from the eruption.

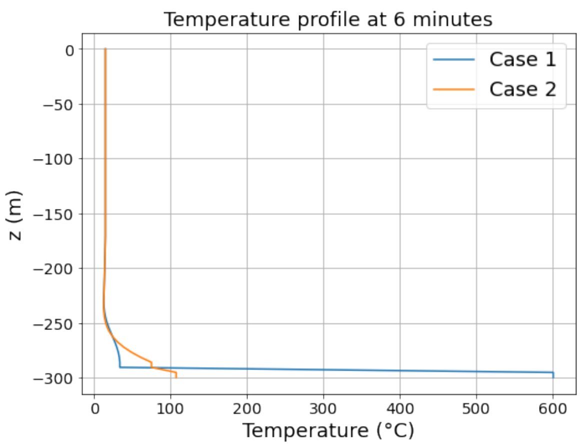

Figure 4: Temperature profile above the volcano for case 1 and 2 at 6 minutes.

https://doi.org/10.5194/egusphere-2025-6265
Preprint. Discussion started: 6 January 2026

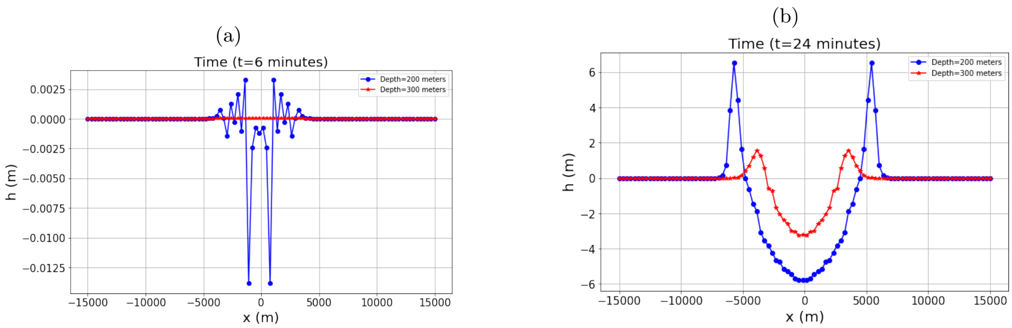

Figure 5: Surface wave elevation for the cases with variable depth and fixed heat flux.

References

[Kanojia et al., 2023] Kanojia, M., Gurusamy, S., and Basu, B. (2023). Modeling of tsunami generated in stratified oceans by sub-aquatic volcanic eruptions. *Physics of Fluids*, 35(5).

[Kedrinskii, 2005] Kedrinskii, V. (2005). *Hydrodynamics of Explosion: experiments and models*. Springer Science & Business Media.

[Le Méhauté and Wang, 1996] Le Méhauté, B. and Wang, S. (1996). *Water waves generated by underwater explosion*, volume 10. World Scientific.

[Lipiejko et al., 2021] Lipiejko, N., Whittaker, C. N., Lane, E., White, J., and Power, W. (2021). Tsunami generation by underwater volcanic explosions: Application to the 1952 explosions of Myojinsho Volcano. *Pure and Applied Geophysics*, 178:4743–4761.

[Liu and Fritz, 2023] Liu, Y. and Fritz, H. (2023). Physical modeling of spikes during the volcanic tsunami generation. *Physics of Fluids*, 35(6).

[Mahadevan et al., 1996a] Mahadevan, A., Oliger, J., and Street, R. (1996a). A nonhydrostatic mesoscale ocean model. part i: Well-posedness and scaling. *Journal of Physical Oceanography*, 26(9):1868–1880.

[Mahadevan et al., 1996b] Mahadevan, A., Oliger, J., and Street, R. (1996b). A nonhydrostatic mesoscale ocean model. part ii: Numerical implementation. *Journal of Physical Oceanography*, 26(9):1881–1900.

[Moore et al., 1966] Moore, J., Nakamura, K., and Alcaraz, A. (1966). The september 28–30, 1965 eruption of Taal Volcano, Philippines. *Bulletin Volcanologique*, 29:75–76.

[Morrissey et al., 2010] Morrissey, M., Gisler, G., Weaver, R., and Gittings, M. (2010). Numerical model of crater lake eruptions. *Bulletin of Volcanology*, 72:1169–1178.

[Muraviev et al., 1998] Muraviev, Y., Fedotov, S., Budnikov, V., Ozerov, A., Maguskin, M., Dvigalo, V., Andreev, V., Ivanov, V., Kartasheva, L., and Markov, I. (1998). Volcanic activity in the Karymsky center in 1996: Summit eruption at Karymsky and phreatomagmatic eruption in the Akademii Nauk Caldera. *Journal of volcanology and Seismology*, 19:567–604.

[Nakano et al., 1954] Nakano, M., Unoki, S., Hanzawa, M., Marumo, R., and Fukuoka, J. (1954). Oceanographic features of a submarine eruption that destroyed the kaiyo-maru no. 5. *Journal of Marine Research*, 13:48–66.

[Nishimura et al., 2005] Nishimura, Y., Nakagawa, M., Kuduon, J., and Wukawa, J. (2005). Timing and scale of tsunamis caused by the 1994 Rabaul eruption, East New Britain, Papua New Guinea. In *Tsunamis*, pages 43–56. Springer.

https://doi.org/10.5194/egusphere-2025-6265
Preprint. Discussion started: 6 January 2026

[Paris, 2015] Paris, R. (2015). Source mechanisms of volcanic tsunamis. *Philosophical Transactions of the Royal Society A: Mathematical, Physical and Engineering Sciences*, 373.

[Paris et al., 2014] Paris, R., Switzer, A., Belousova, M., Belousov, A., Ontowirjo, B., Whelley, P., and Ulvrova, M. (2014). Volcanic tsunami: a review of source mechanisms, past events and hazards in southeast asia (indonesia, philippines, papua new guinea). *Natural Hazards*, 70:447–470.

[Paris and Ulvrova, 2019] Paris, R. and Ulvrova, M. (2019). Tsunamis generated by subaqueous volcanic explosions in Taal Caldera lake, philippines. *Bulletin of Volcanology*, 81:1–14.

[Rossby, 1965] Rossby, H. (1965). On thermal convection driven by non-uniform heating from below: an experimental study. In *Deep Sea Research and Oceanographic Abstracts*, volume 12, pages 9–16. Elsevier.

[Rossby, 1998] Rossby, T. (1998). Numerical experiments with a fluid heated non-uniformly from below. *Tellus A: Dynamic Meteorology and Oceanography*, 50(2):242–257.

[Schindelé et al., 2024] Schindelé, F., Kong, L., Lane, E., Paris, R., Ripepe, M., Titov, V., and Bailey, R. (2024). A review of tsunamis generated by volcanoes (tgv) source mechanism, modelling, monitoring and warning systems. *Pure and Applied Geophysics*, pages 1–48.

[Torsvik et al., 2010] Torsvik, T., Paris, R., Didenkulova, I., Pelinovsky, E., Belousov, A., and Belousova, M. (2010). Numerical simulation of a tsunami event during the 1996 volcanic eruption in Karymskoye lake, Kamchatka, Russia. *Natural Hazards and Earth System Sciences*, 10:2359–2369.